Aberrant Endometrial Features of Pregnancy in Diabetic NOD Mice

Suzanne D. Burke, Hongmei Dong, Aleah D. Hazan, and B. Anne Croy

OBJECTIVE—Pregnant diabetic women are at a 4–12 times higher risk for preeclampsia, an urgent acute-onset complication of mid- to late gestation, than normal pregnant women. Hallmarks of preeclampsia are hypertension, proteinuria, and incomplete modification of endometrial spiral arteries. Transient proangiogenic lymphocytes called uterine natural killer (uNK) cells are implicated in human and rodent spiral artery modification. We studied mid- to late gestations in spontaneously type 1 diabetic NOD mice to investigate whether diabetes alters uNK cell homing and/or function.

RESEARCH DESIGN AND METHODS—Normoglycemic, prediabetic, and diabetic NOD mice and controls were mated. Lymphocytes and endometrial endothelium and decidua were studied histologically and in functional assays.

RESULTS—Conception accelerated progression to overt diabetes in NOD females who had limited spiral artery development, heavier placentas, and lighter fetuses displaying numerous birth defects compared with controls. UNK cell numbers were reduced in the decidua basalis of diabetic females, whereas interferon-γ production was elevated. In diabetic NOD mice, decidual expression of the mucosal vascular addressin cell adhesion molecule (MAdCAM)-1 was aberrant in position, whereas vascular cell adhesion molecule (VCAM)-1 expression was reduced. Assays of lymphocyte adhesion to tissue sections under shear forces indicated that diabetes compromises the potential homing functions of both endometrial endothelium and peripheral NK cells.

CONCLUSIONS—In diabetes, gestational endometrium has immune and vascular defects that likely contribute to murine fetal loss and birth defects. Analogous problems and preeclampsia in diabetic women may involve similar mechanisms. ***Diabetes* 56: 2919–2926, 2007**

The NOD mouse is a well-characterized model of type 1 diabetes (rev. in 1). NOD mice develop spontaneous T-cell–mediated autoimmune insulitis, followed by diabetes that is clinically and genetically similar to human disease (rev. in 2 and 3). Disease progression is associated with a gain in islet expression of leukocyte homing molecules such as mucosal vascular addressin cell adhesion molecule (MAdCAM)-1 and vascular cell adhesion molecule (VCAM)-1 (4). Immune dysfunctions in NOD mice include altered regulatory T-cells (5–7) and functional as well as numerical deficits in NK and NKT cells (8,9). Despite a wealth of information on NOD mice, study of their reproductive biology is limited. Fetal consequences of maternal diabetes are described. These include death, birth defects, and potential for early development of type 1 diabetes in offspring (10–12). Whereas normoglycemic NOD mice are excellent breeders (1), features of mid-gestation implantation sites in overtly diabetic mice are unknown.

Human pregnancies complicated by diabetes have a three- to ninefold increased risk of fetal/neonatal morbidity and mortality (13). These risks include death, intrauterine growth restriction, neural tube defects, premature birth, and macrosomia (14). Risks are reduced but not eliminated by optimal maternal glycemic control, indicating a complex etiology. Histologically, placentas from diabetic women show evidence of hypoxia (increased nucleated fetal erythrocytes) and immature villi with increased fibrinoid deposition (15). The supporting maternal vasculature is increased in length (16) but shows wall hyperplasia with lumen stenosis (16) and incomplete spiral artery modification (17). Diabetes increases the risk of preeclampsia, a serious complication of pregnancy of unknown etiology, 12-fold (18). Preeclampsia presents as hypertension and proteinuria and, without intervention, can develop into HELLP syndrome (hemolysis, elevated liver enzymes, and low platelets) and eclampsia (convulsions). HELLP syndrome has significant maternal morbidity and mortality. Currently, the only successful treatment for preeclampsia is delivery of the placenta. Preeclampsia is a multifactorial disease with immune, genetic, and environmental contributions. Histologically, hallmarks of preeclampsia are poor placentation, with hypoxic signs, and incomplete spiral artery modification (19).

Uterine natural killer (uNK) cells are a terminally differentiated NK cell subset that proliferate in the uteri of many species early in pregnancy (20). Functions of uNK cells are still under investigation but include production of angiogenic factors (21,22). In mice, uNK cell–derived interferon (IFN)-γ is the established initiator of gestational spiral artery modification. The structural changes, called "spiral artery modification," create large-volume low-pressure vessels feeding into placentas. These changes are completed histologically in mice by midpregnancy (gestation day [gd] 10 of a 19- to 20-day term [23]). Transplantable uNK progenitor cells are not found in mouse uteri but occur in all peripheral lymphoid tissues (24). Although hematopoeitic stem cells occur in human uteri (25), in vitro assays show that human $CD56^{bright}$ blood NK cells, the minor blood NK cell type, gain in functional interactions with endothelium of the decidua basalis at the

From the Department of Anatomy and Cell Biology, Queen's University, Kingston, Ontario, Canada.

Address correspondence and reprint requests to Suzanne Burke, Department of Anatomy and Cell Biology, Queen's University, Kingston, Ontario, Canada K7L 3N6. E-mail: 5sb28@queensu.ca.

Received for publication 6 June 2007 and accepted in revised form 4 September 2007.

Published ahead of print at http://diabetes.diabetesjournals.org on 7 September 2007. DOI: 10.2337/db07-0773.

gd, gestation day; HPF, high-power field; IFN, interferon; MAdCAM, mucosal vascular addressin cell adhesion molecule; MLAp, mesometrial lymphoid aggregate of pregnancy; PNAd, peripheral lymph node addressin; uNK, uterine natural killer; VCAM, vascular cell adhesion molecule; VEGF, vascular endothelial growth factor.

preovulatory menstrual cycle surge in luteinizing hormone. This gain in potential for NK cell egress into decidua predicts uterine receptivity for transferred embryos (26) and is consistent with the dominance of $CD56^{bright}$ NK cell subset in decidua (27).

Diabetes is associated with defects in NK cell function and alterations in lymphocyte chemotaxis. We hypothesized that the incomplete spiral arterial remodeling of diabetic human pregnancies is due, at least in part, to decoy homing of uNK cells to the inflamed pancreas and/or reduced uNK cell function. The goal of this study was to characterize implantation sites in normoglycemic, pre-diabetic, and diabetic NOD mice at mid-gestation.

RESEARCH DESIGN AND METHODS

NOD/LtJ, NOD/LtSz-*scid.scid* (NOD.*scid*), C56Bl/6J (B6), and FVB/NJ (FVB) male and female mice were purchased from The Jackson Laboratory (Bar Harbor, ME). C57BL/6N (B6) mice and BALB/c mice were purchased from Taconic Farms (Germantown, NY). NOD and NOD.*scid* mice were housed in a barrier facility; B6 and FVB mice were housed conventionally. From 9 weeks of age, NOD mice were monitored weekly for hyperglycemia using tail venipuncture and OneTouch Ultra Glucose meter and strips (LifeScan, Burnaby, British Columbia, Canada). NOD mice were classified as normoglycemic (<11 mmol/l), pre-diabetic (11.1–14.9 mmol/l), and diabetic (≥15 mmol/l on sequential measurements). Experimental design precluded developing a diabetes incidence curve for females in our NOD colony. The diabetes incidence for males was >50% at 30 weeks of age ($n = 8$), consistent with published work (1).

Female NOD and NOD.*scid* mice with known blood glucose were paired with normoglycemic NOD males to obtain pregnancies. Copulation plug detection was named gd0. Gd-matched pregnancies in syngeneically mated B6, NOD.*scid*, FVB, and BALB/c mice were used as controls. Mice were killed at gd6 and gd8 for immunohistochemistry, gd7 for adhesion assays, or gd10 for morphometric analyses and quantification of IFN-γ. Peripartum placentas and offspring were weighed.

Avertin-anesthetized mice were killed by cervical dislocation. For histology, pancreas and uterus were dissected and fixed in fresh 4% neutral buffered paraformaldehyde (Sigma-Aldrich, Oakville, Ontario, Canada). For adhesion assays, these tissues plus multiple peripheral lymph nodes (cervical, submandibular, axial, mesenteric, iliac, superficial inguinal, and popliteal) were dissected, embedded in cryomatrix (Shandon Cryomatrix, Thermo Fisher Scientific, Waltham, MA), and snap frozen in liquid nitrogen. All animal usage complied with protocols approved by Queen's University's Animal Care Committee.

Histology

Morphometry. Paraformaldehyde-fixed implantation sites were processed using an automatic tissue processor (Triangle Biomedical Sciences, Durham, NC) and paraffin embedded using standard methods (28). For each group, three implantation sites from three dams were serial sectioned at 7 μm. At least 77 sections were cut at the center of each implantation site and mounted to glass slides. Alternate slides were stained with hematoxylin and eosin for vessel morphometry or periodic acid Schiff reagent for uNK cell enumeration. Eleven sections, at least 42 μm apart (to avoid duplicate enumeration of uNK cells), were scored per implantation site. UNK cells were enumerated within a standardized surface area in each of decidua basalis and mesometrial lymphoid aggregate of pregnancy (MLAp), a transient lymphoid structure between the circular and longitudinal smooth muscle coats of the uterus. Spiral artery wall and lumen diameters were measured and expressed as wall–to–lumen diameter ratios. When present in the tissue, three spiral artery cross-sections were measured on each of the 11 sections from each implantation site. All analyses were performed using an AxioImager M.1 microscope and Axiovision software (Carl Zeiss, Oberkochen, Germany).

Immunohistochemistry. Indirect antibody staining was performed for peripheral lymph node addressin (PNAd), MAdCAM-1, and VCAM-1 on paraffin-embedded sections of pancreas and uterus from virgin, gd6, or gd8 normoglycemic NOD mice; diabetic NOD mice; and B6 mice. Three viable implantation sites and six representative sections per antibody were used, plus isotype controls. Sections were deparaffinized, followed by antigen retrieval for MAdCAM-1 and VCAM-1 (citrate buffer and proteinase K methods, respectively). Endogenous peroxidase was quenched with 0.3% H_2O_2 (30 min), followed by blocking with 10% normal rabbit serum in 1% BSA (1 h). Primary antibodies were incubated overnight at 4°C (biotinylated rat anti-mouse PNAd, 1:100, MECA-79 [Biolegend, San Diego, CA]; LEAF-purified rat anti-mouse MAdCAM-1, 1:100, MECA-367 [Biolegend]; rat anti-mouse VCAM-1, 1:20, MK-2 [Antigenix America, Huntington Station, NY]). MAdCAM-1 and VCAM-1 sections were incubated with rabbit anti-rat IgG biotinylated secondary antibody (1:100; Vector Labs, Burlingame, CA) (30 min). All sections were subjected to amplification with Vectastain Elite ABC kit (Vector Labs) and diaminobenzidine substrate for visualization.

Lymphocyte adhesion to frozen tissue under shear forces. Cryostat sections (12 μm) of substrate tissue (mouse lymph nodes, pancreas, and gd7 uterus) were cut immediately before use in the modified Stamper-Woodruff adhesion assay. Two sources of indicator lymphocytes were used: human peripheral blood lymphocytes or mouse splenocytes. Human blood in ACD anticoagulant (BD Biosciences, San Jose, CA) was provided by a healthy nulliparous noncycling adult female using depot-medroxyprogesterone acetate contraception. This donor had normal random and fasting blood glucose, insulin, and lipid profiles. Peripheral blood lymphocytes were isolated as previously described (24,29), adjusted to 5×10^6 cells/μl in serum-free RPMI and incubated with anti-CD56 mAb (1:100; Coulter Immunology, Hialeah, FL).

Mouse splenocytes were dissociated mechanically, erythrocytes were lysed, and lymphocytes were harvested after centrifugation over Lympholyte-M (Cedarlane Laboratories, Burlington, Ontario, Canada). Aliquots of 5×10^6 cells/100 μl in RPMI and labeled with either anti-CD49b mAb (DX5, 1:100; eBioscience, San Diego, CA) or CellTracker Blue CMAC (Molecular Probes; Invitrogen, Burlington, Ontario, Canada), a fluorescent intravital dye without effects on adhesive function (30).

To assess changes in endothelial cell function induced by diabetes, aliquots of PE-Cy5-CD56–labeled human peripheral blood lymphocytes were overlaid onto sections of normoglycemic or diabetic NOD pancreas, lymph nodes, or gd7 uterus or matched B6 tissues on a rotating table (112 rpm) and incubated (30 min, 4°C). Nonadherent cells were removed by dipping the slides into PBS; slides were then fixed (4% paraformaldehyde, 30 min), rinsed (PBS then dH_2O), and mounted. Fluorescent adherent cells were scored in 25 high-power fields (HPF)/specimen at ×400 magnification.

To assess changes in lymphocyte function with progression to diabetes, B6 substrate tissues were incubated with splenocytes from normoglycemic or diabetic NOD mice or B6 mice. The experiment was conducted as above.

IFN-γ quantification. Uteri were collected from virgin or gd10 normoglycemic, pre-diabetic, or diabetic NOD mice and from a gd10 BALB/c mouse. The MLAp and decidua basalis were dissected from healthy implantation sites; each was pooled by uterus in a microcentrifuge tube containing 100 μl RPMI and homogenized by Kontes micropestle (Fisher Scientific, Waltham, MA). Mesometrial tissue was dissected from virgin mice and handled similarly. After centrifugation (800*g*; 5 min), supernatants were collected and stored at −20°C until assayed for IFN-γ by enzyme-linked immunosorbent assay as previously described (31). The limit of detection of this assay was 0.01 IU IFN-γ.

Statistical analysis. Data were analyzed using the Prism 4.03 Statistical Software package (GraphPad, San Diego, CA) and are presented as means ± SE. Blood glucose values were analyzed by repeated-measures ANOVA, followed by both linear trend and Bonferroni's test. Fetal and placental weights were analyzed by independent one-tailed t tests. Resorption rates, MLAp uNK counts, spiral artery lumen diameters, and adhesion assays were analyzed using ANOVA with Bonferroni's post-test. The Kruskal-Wallis test was used to analyze uNK counts within the decidua basalis, IFN-γ quantification, and spiral artery wall–to–lumen ratios, followed by Dunn's post-test. A P value <0.05 was considered statistically significant.

RESULTS

Pregnancy accelerates progression to overt diabetes. Pregnant mammals develop mild glucose intolerance at mid-gestation to elevate fetal glucose availability. In normal mice, blood glucose increases at gd4.5 (32). All pregnant NOD mice (normoglycemic, $n = 5$; pre-diabetic, $n = 7$; diabetic, $n = 7$) displayed significant increases in blood glucose from their individual baselines (three prior measurements; Fig. 1) ($P < 0.005$). Mean gd10 blood glucose values were significantly increased only in mice overtly diabetic (19.30 ± 4.352 vs. normoglycemic 6.885 ± 0.8947 and pre-diabetic 7.950 ± 1.698) before mating ($P < 0.005$).

Fetal outcomes during diabetic pregnancy. The impact of diabetes on NOD fetuses was scored grossly (Table 1). Diabetic mice ($n = 4$) had significantly more resorption sites than normoglycemic ($n = 3$), pre-diabetic ($n = 6$), and NOD.*scid* ($n = 3$) mice at gd10 ($P = 0.021$). However,

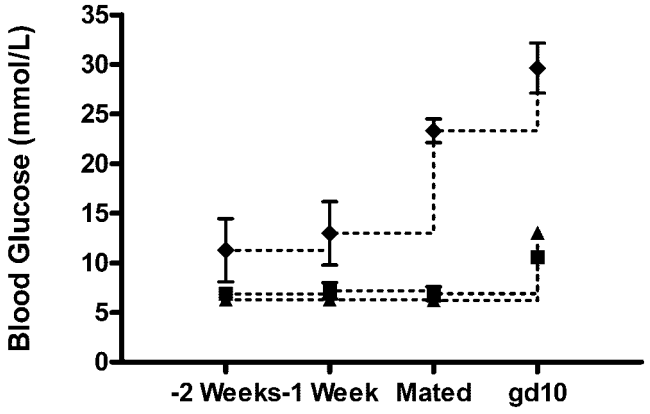

FIG. 1. Blood glucose values of mated NOD mice. Mice were classified as normoglycemic (n = 5; ■; <11 mmol/l), pre-diabetic (n = 7; ▲; >11.1–14.9 mmol/l), or diabetic (n = 7; ♦; >15 mmol/l) based on values measured at gd10. Pregnancy elevated blood glucose values in all animals, with the largest increase in diabetic mice before conception. Diabetic NOD mice showed an increase in blood glucose from three previous measurements (P < 0.005).

gross study underestimated losses in diabetic NOD mice, since additional resorptions were found histologically. Weights of gd18 fetuses and placentas from one overtly diabetic NOD dam (n = 1) were compared with fetal weights from FVB dams (n = 3). NOD placental weight was significantly greater than FVB placental weight (0.13 ± 0.0080 vs. 0.086 ± 0.0031 g, $P < 0.0001$). Although NOD placental weights were greater, morphometry revealed a smaller, more compact placental area than FVB placentas (data not shown).

Fetuses from the diabetic NOD dam were smaller than those from FVB dams (0.98 ± 0.065 vs. 1.22 ± 0.068 g, $P < 0.05$). FVB fetuses included one that was very underweight but had no gross abnormalities and another fetus with agnathia. In contrast, NOD fetuses had gross neural tube defects (spina bifida and exencephaly, n = 3) and growth restriction (Fig. 2). Further necropsy revealed additional defects including situs inversus, diaphragmatic hernia, agnathia, anopthalmia, cardiac hypertrophy, pancreatic hyperplasia, asplenia, and an occult spina bifida. Each NOD fetus had at least one defect, whereas most, as reported by others (10,11), had multiple defects.

uNK cells in NOD pregnancy. In NOD.*scid* (n = 3) and normoglycemic NOD mice (n = 3), uNK cell numbers in the MLAp (site of most uNK cell proliferation) and decidua basalis (site dominated by postmitotic uNK cells) were consistent with published numbers in normal mice (33). Pre-diabetic (n = 3) and diabetic NOD mice (n = 3) had reduced uNK cell numbers in the MLAp (81.9 ± 1.18; 80.8 ± 1.02) compared with NOD.*scid* mice (87.5 ± 2.22) ($P < 0.05$, Fig. 3). Diabetic NOD mice had drastically reduced decidual uNK numbers compared with all other groups (26.1 ± 0.67) ($P < 0.001$). Decidual uNK cells were small and had limited cytoplasmic granularity, suggesting immaturity.

TABLE 1
Fetal loss rate in NOD mice

	Blood glucose at gd10	Number of dams	Total embryos	% Resorption
NOD.*scid*	9.6	3	31	6.3
Normoglycemic NOD	10.2	3	32	4.0
Pre-diabetic NOD	13.3	6	71	9.5
Diabetic NOD	26.9*	4	40	30.3†

*$P < 0.0005$, †$P = 0.021$ compared with pre-diabetic, normoglycemic, and NOD.*scid* mice.

To further assess uNK cell function in NOD mouse implantation sites, IFN-γ was quantified in the MLAp and decidua basalis. gd10 BALB/c (n = 1) MLAp and decidua basalis were positive controls, and IFN-γ concentrations matched a previous report for immune-competent mice (9.04 and 12.92, respectively) (31). Mesometrial uterus from a virgin normoglycemic NOD (n = 1) mouse lacked IFN-γ, a finding typical of virgin uteri from normal mice. IFN-γ concentrations in decidua basalis and MLAp from normoglycemic (n = 3) and pre-diabetic NOD (n = 3) mice did not differ. However, IFN-γ concentration within the decidua basalis of diabetic NOD mice (n = 3) was significantly higher than in decidua basalis from normoglycemic NOD mice (34.01 ± 4.47 vs. 9.35 ± 3.74, $P < 0.05$). No difference in IFN-γ concentration within the MLAp was found between normoglycemic NOD, pre-diabetic NOD, and diabetic NOD mice.

Spiral artery modification in diabetic NOD mice. Fewer spiral arteries were found in implantation sites from pre-diabetic (n = 3) and diabetic NOD (n = 3) mice than in normoglycemic NOD (n = 3) or NOD.*scid* mice (n = 3). Spiral artery lumen diameters shortened as blood glucose increased. For arteries in pre-diabetic (26.45 ±

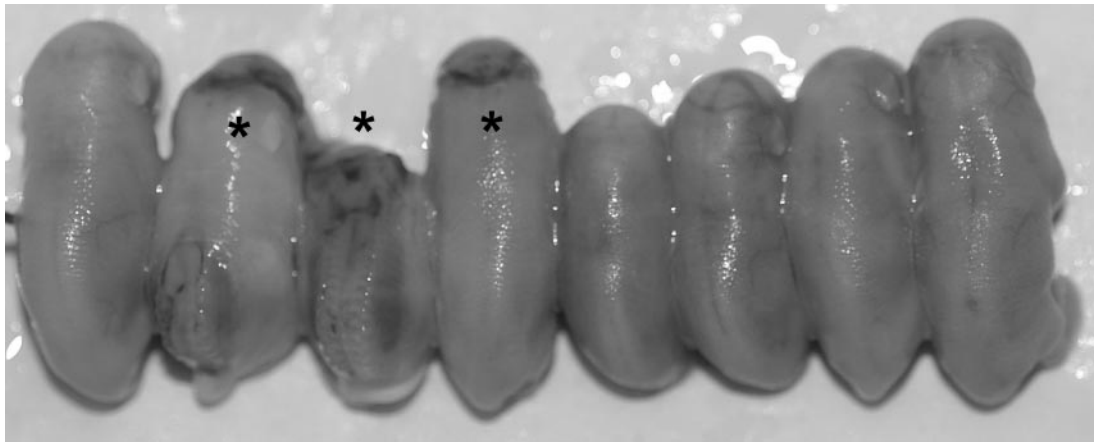

FIG. 2. A litter of gd18 fetuses born to an overtly diabetic NOD dam. Three neural tube defects and widely variable fetal size were noted. At necropsy, only 50% had the potential to survive, all exhibited congenital defects.

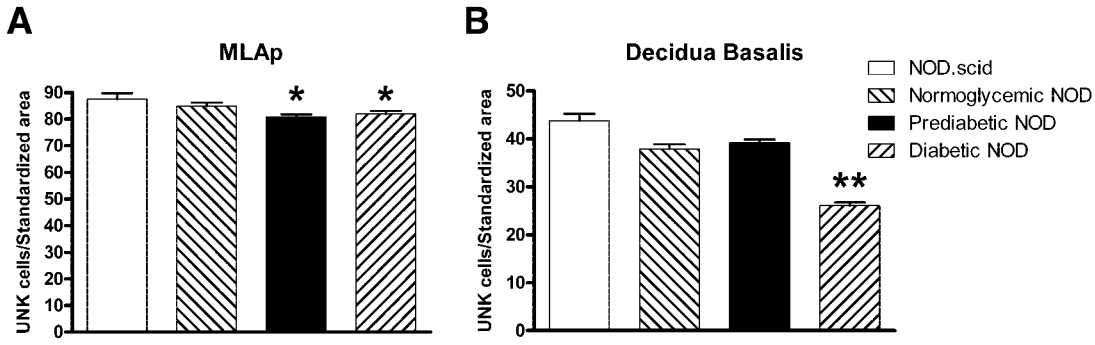

FIG. 3. uNK cell counts within the (*A*) MLAp and (*B*) decidua basalis of NOD.*scid*, normoglycemic, pre-diabetic, and diabetic NOD implantation sites. **P* < 0.05 compared with NOD.*scid* implantation sites. ***P* < 0.001 compared with normoglycemic and pre-diabetic NOD implantation sites. Data are means ± SE from *n* = 3 mice per group (three viable implantation sites per mouse).

0.62 μm) and diabetic dams (23.36 ± 0.57 μm), values were statistically different compared with normoglycemic NOD (36.82 ± 1.04 μm) or NOD.*scid* mice (34.43 ± 0.81 μm) ($P < 0.001$) (Fig. 4*A*). Spiral arterial wall-to-lumen diameter ratios for normoglycemic NOD mice and NOD-*.scid* mice were greater than reported for B6 mice (34). This may indicate a basal arterial defect in the NOD strain. Spiral arteries from pre-diabetic (3.33 ± 0.092) and diabetic NOD mice (3.82 ± 0.11) had even greater wall-to-lumen ratios than normoglycemic NOD (2.39 ± 0.058) and NOD.*scid* mice (1.82 ± 0.044), suggesting progressive loss of capacity for spiral artery modification with increasing hyperglycemia ($P < 0.01$) (Fig. 4*B*).

Localization of endothelial cell addressins. To determine if decidua basalis of diabetic NOD mice expressed addressins aberrantly, PNAd, MAdCAM-1, and VCAM-1 were localized at gd6 and gd8. PNAd was not significantly detected in any implantation sites. MAdCAM-1 was localized to the lateral sinusoids in B6 ($n = 3$), while, in NOD mice ($n = 3$), reactivity was found in antimesometrial decidua. VCAM-1 was strongly expressed in the central decidua, mesometrial, and antimesometrial decidua of B6 mice (Fig. 5*A*). VCAM-1 was similarly localized in NOD mice, but staining intensity was weaker (Fig. 5*B*).

PNAd, MAdCAM-1, and VCAM-1 expression was absent from pancreatic islets from pregnant B6 mice (Fig. 5*C*). Moderate expression of PNAd, MAdCAM-1, and VCAM-1 was observed in islets from pregnant normoglycemic NOD mice. These molecules were strongly expressed in some of the islets remaining in pregnant diabetic NOD mice (Fig. 5*D*).

Endothelial cell function in NOD uterus and pancreas. To assess endothelial homing receptor function, CD56-tagged indicator lymphocytes were evaluated for adhesion to various tissues. Adhesion to lymph nodes was used as a positive control and was similar for normoglycemic NOD ($n = 8$), diabetic NOD ($n = 10$), and B6 ($n = 6$) substrates (Fig. 6). Adhesion to diabetic NOD pancreas (5.28 ± 1.03 cells/HPF) was greater than to B6 pancreas (1.58 ± 0.19 cells/HPF) ($P < 0.05$). Low adhesion to B6 pancreas is consistent with published data. Adhesion to B6 uterus was localized to decidua basalis and low, concurring with previous reports for donors not at the ovulatory stage of their menstrual cycle (35). Adhesion to normoglycemic NOD uterus (13.9 ± 3.3 cells/HPF) was greater than to diabetic NOD (6.7 ± 0.50 cells/HPF) or B6 uterus (3.46 ± 0.54 cells/HPF) ($P < 0.05$). $CD56^+$ cells showed less localized binding to decidua basalis in decidual sections from diabetic NOD mice: cells bound to uterine glands, antimesometrial decidua, and myometrium. Comparisons to controls used only cells bound to decidua basalis.

NOD lymphocyte recognition of vascular addressins. Fluorescently tagged splenic NK cells from diabetic NOD mice ($n = 2$) showed significantly more adhesion to normal B6 ($n = 2$) peripheral lymph nodes (6.28 ± 0.24 vs.

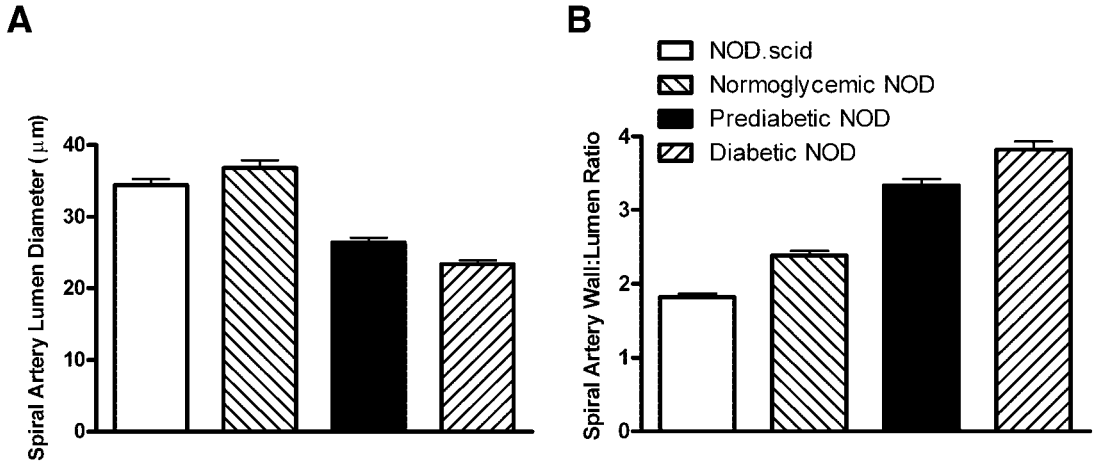

FIG. 4. *A*: Spiral artery lumen diameter (μm) in NOD.*scid*, normoglycemic, pre-diabetic, and diabetic NOD mice at gd10. *B*: Wall-to-lumen ratios of spiral arteries in NOD.*scid*, normoglycemic, pre-diabetic, and diabetic implantation sites. All groups are significantly different ($P < 0.05$), except for NOD.*scid* versus normoglycemic NOD mice. Data are means ± SE from *n* = 3 mice per group (three viable implantation sites per mouse).

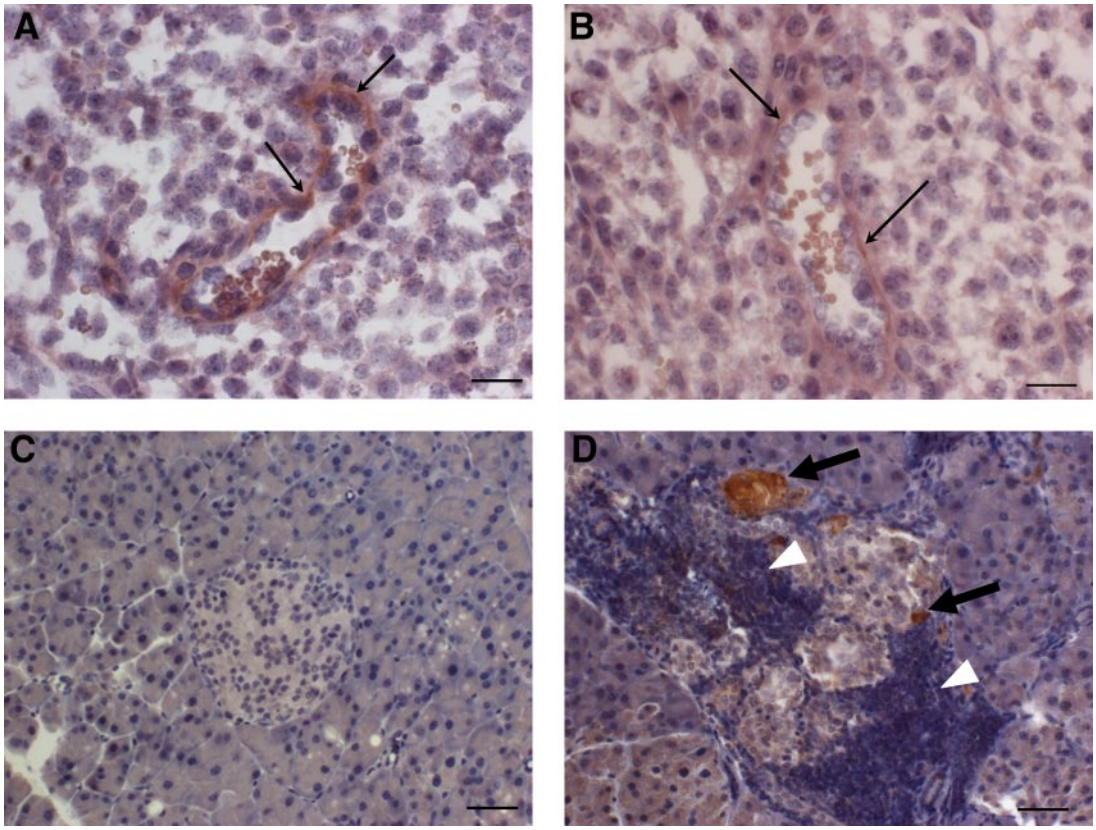

FIG. 5. Representative VCAM-1 staining in gd8 mouse tissues. Endothelium in vessels of decidua basalis consistently appeared more reactive in B6 mice (arrow) (*A*) than in diabetic NOD mice (arrow) (*B*). Pancreatic islets of B6 mice were unreactive (*C*) but were strongly reactive in diabetic NOD mice (arrow) (*D*). The latter showed leukocyte infiltration (arrowhead), consistent with insulitis observed in overt diabetes. Tissues illustrated are from paired single donors. Counterstained with hematoxylin. Bar = 20 μm. (Please see http://dx.doi.org/10.2337/db07-0773 for a high-quality digital representation of this figure.)

3.46 ± 0.38 cells/HPF) ($P < 0.05$) (Fig. 7*A*). Adhesion of splenic NK cells from NOD mice (diabetic NOD, 4.80 ± 0.0050 cells/HPF; normoglycemic NOD, 3.39 ± 0.43 cells/HPF) to B6 pancreatic endothelium, regardless of blood glucose, was increased over NK cells from B6 mice (1.84 ± 0.0040 cells/HPF) ($P < 0.05$). There were no differences between the three splenic NK cell populations in adhesion to gd7 B6 uterus.

In these experiments, total (CMAC-stained) splenocyte binding was enumerated on adjacent tissue sections to enable calculation of NK cell enrichment (Fig. 7*B*). About 10% of the splenocytes from B6 and normoglycemic NOD mice adhering to B6 lymph nodes and pancreas were $DX5^+$ NK cells. In diabetic NOD mice, the proportional binding of NK cells increased to B6 lymph nodes (30.7 ± 4.27%) and was significant in pancreas (51.5 ± 18.1%) ($P < 0.05$). The proportion of $DX5^+$ B6 splenocytes binding to B6 uterine endothelium was high (67.0 ± 0.88%). This proportion was lower for splenocytes from normoglycemic NOD mice (33.4 ± 9.12%) and was significantly different for diabetic NOD mice (27.1 ± 2.81%) ($P < 0.05$). This suggests that NK cells from diabetic mice are reduced in ability to engage with uterine endothelium for extravasation and that other cell types compete for these receptors. This may skew the immune cell populations at a diabetic maternal-fetal interface.

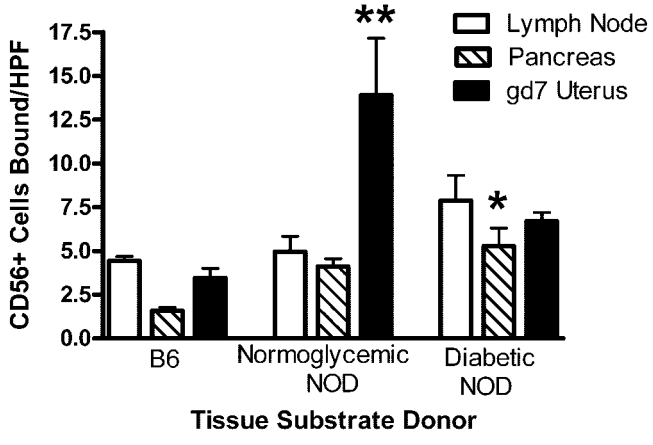

FIG. 6. Human $CD56^+$ cells bound to peripheral lymph node from B6, normoglycemic NOD, pre-diabetic NOD, or diabetic NOD mice per high-powered field (×400 magnification). Data are presented from replicate experiments using the same blood donor. *$P < 0.05$ vs. B6, **$P < 0.05$ vs. B6 and diabetic NOD mice.

DISCUSSION

This study addressed whether reduced uterine homing and/or function of NK cells occurs in diabetic pregnancy that would impair pregnancy-associated spiral arterial modification and link endometrial lymphocytes to the pregnancy complications of diabetic women. Spontaneous disease in type 1 diabetic NOD mice was used as a model for gradual disease progression. Unexpectedly, defective spiral arterial development and modification were found in normoglycemic NOD and NOD.*scid* mice. This pathology is absent in implantation sites of pregnant *scid* mice, which lack T- and B-cells (36). NOD.*scid* mice have similar

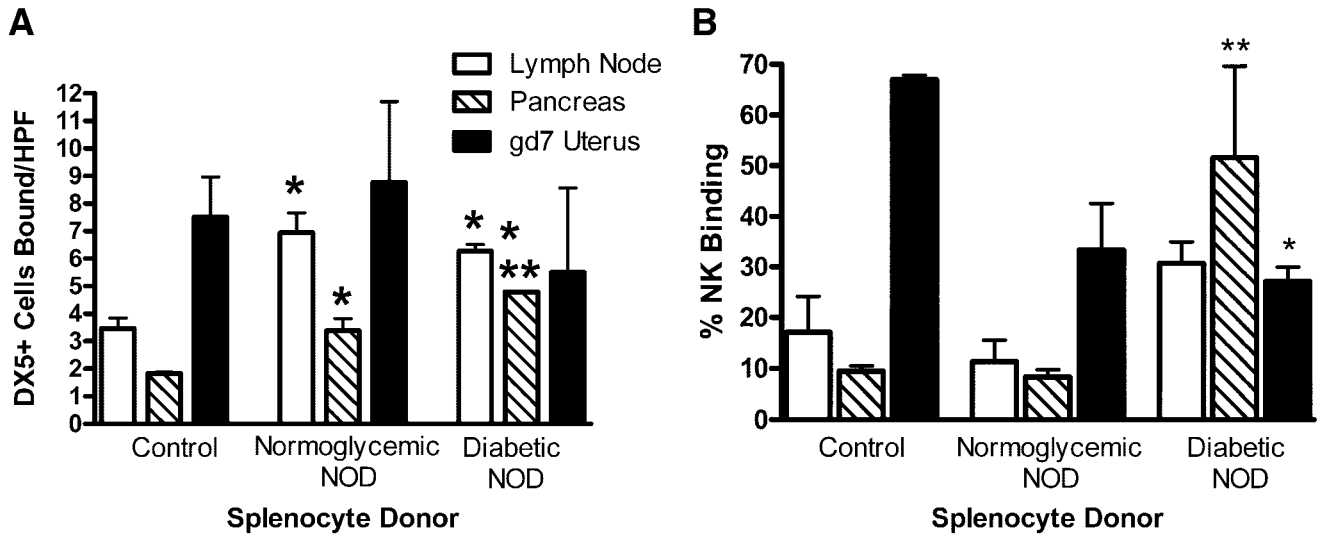

FIG. 7. FITC-DX5$^+$ splenic NK cells (*A*) or DX5$^+$/CMAC$^+$ splenic NK/lymphocytes (*B*) bound to peripheral lymph node, pancreas, or gd7 uterus from normal B6 mice per high-powered field (×400 magnification). Splenocyte donors are B6, normoglycemic NOD, or diabetic NOD mice. *P < 0.05 vs. B6, **P < 0.05 vs. B6 and normoglycemic NOD splenocyte binding.

NK cell defects to NOD mice but do not develop insulitis or diabetes. Of particular note was the paucity of spiral arteries, which are major vessels, in NOD implantation sites. This has not been reported in other strains. Reduced neovascularization has been reported in NOD mice subjected to femoral artery ischemia. This was attributed to lower induction of vascular endothelial growth factor (VEGF) in ischemic NOD tissue (37). VEGF (38) and the VEGF family member placental growth factor (PlGF) (39) are major uNK cells products. In other tissues, VEGF regulates the expression of chemokine ligands that position recruited bone marrow–derived circulating cells (40) and promote flexible (i.e., not developmentally hardwired) angiogenesis. Endometrium requires flexible angiogenesis, since the number of arriving blastocysts is variable between reproductive cycles. The vascular histopathology was more severe in pre-diabetic and diabetic NOD mice (5,41).

Progesterone, the essential hormone of pregnancy, and IFN-γ are among the regulators of VEGF transcription (42,43). Progesterone is absolutely required for terminal uNK cell differentiation, and uNK cells are the major source of mouse implantation site IFN-γ during the first half of gestation. Because spiral artery modification in mice is normally initiated by IFN-γ released from uNK cells (36,44), this cytokine was quantified in implantation sites. As in other strains, IFN-γ was not detected in virgin uterus but was present between gd6 and gd10 in NOD implantation sites. Levels were comparable to those in a normal mouse and consistent with our earlier published data (31), except in the decidua basalis of overtly diabetic gd10 females. This tissue, in which uNK cells are reduced, unexpectedly showed elevated IFN-γ. This finding suggests that the primary deficit in spiral artery development in NOD mice is not overcome by the influx of IFN-γ–producing uNK cells. The elevated IFN-γ that we saw may relate to the disease stage we studied. Rodacki et al. (45) showed, in type 1 diabetic patients, numbers and activation status of blood NK cells vary with disease stage. At onset, NK cells are reduced but unusually activated producers of IFN-γ. With longer-standing disease, both patients and NOD mice lose NK cell activation receptors (45,46). Because spontaneously diabetic NOD mice are fragile, usually older than mice used for first pregnancy studies, and prescribed for removal from breeding colonies, we bred our mice as soon as they became diabetic. This may have been in the interval of elevated NK cell activation. We attempted support of diabetic females by subcutaneously implanted slow release insulin rods before mating. This normalized blood glucose only until mating. By gd10, all insulin-treated females had reverted to hyperglycemia (n = 6; S.D.B., B.A.C., unpublished data).

Changes in patterns of vascular addressins are found in diabetic NOD mice (4,47), but effects of pregnancy on these molecules have not been addressed nor have comparisons of expression been made between gestational endometrium and pancreas. We found alterations in the normal pattern of MAdCAM-1 and VCAM-1 expression within the early gestational uterus of diabetic NOD mice. MAdCAM-1 was expressed in an aberrant location, and VCAM-1 expression was less intense. VCAM-1 is thought to be the key addressin in early uNK cell recruitment to deciduas basalis (48). The successful localization of many uNK cells in diabetic NOD pregnancy supports this postulate (48). Homing receptor elevation underlies insulitis, which is present in all adult NOD mice, regardless of diabetic state. Assays of lymphocyte adhesion using NOD pancreas showed that, in pregnancy, as in nonpregnant NOD mice, hyperglycemia elevates islet adhesion (49). The pattern of lymphocyte adhesion to decidualized uterus was less straightforward. There was a striking increase in the level of adhesion to uterus from normoglycemic NOD mice relative to controls. One interpretation of these data is that endometrial endothelium in gestational uterus compensates against pancreatic endothelial cell recruitment signals early in disease but cannot sustain this state as disease progresses. Adhesion assays using NOD splenocytes on B6 tissue showed diabetes-promoted gains in the ability of lymphocytes to adhere to pancreas and peripheral lymph nodes but not to uterus. This is consistent with the relatively normal numbers of uNK cells quantified within gd6–8 implantation sites. It also suggests there is a large reserve of circulating NK cells with tissue-homing potential enabling NK cell elevation in one tissue without

decoy homing from another tissue. Previous studies of normal lymphocytes reported NK cell enrichment among cells adhering to gd7 uterus (26). Similar enrichment was not observed in assays using splenocytes from diabetic NOD mice. Splenic NK cells from diabetic NOD mice were enriched, however, by adhesion to pancreas, suggesting preferential homing to this organ over pregnant uterus.

In human diabetic pregnancy, placental and neonatal sizes are usually correlated; diabetic women frequently having abnormally large placentas with macrosomic infants. The diabetic NOD placentas were abnormally heavy, but fetal trophoblastic areas were greatly reduced relative to maternal decidua basalis in all pregnant NOD and NOD.*scid* mice. Human pregnancies complicated by both diabetes and intrauterine growth restriction or preeclampsia often display hypercellular placental histopathology accompanying small size. Human pregnancies complicated by diabetes have various vasculopathies, which tend to perturb spiral artery modification. Most frequently, long nonspiraling arteries persist that remain responsive to vasoactive substances. In pathological diabetic pregnancies (i.e., comorbid preeclampsia or intrauterine growth restriction), spiral arteries are incompletely modified, resulting in placenta hypoxia. Depending on the timing of the insult, placental insufficiency and/or hypoxia can result in growth restriction or abnormal organ development, intrauterine death, or fetally programmed risk for postnatal health impairment. Fetuses of overtly diabetic NOD dams showed early and late resorption, growth restriction, and a high rate of developmental defects. Our study shows there are major endometrial contributions associated with pathogenesis that include poor vascular bed development and altered endometrial lymphocyte recruitment and function, particularly of proangiogenic uNK cells. Thus, gestation in spontaneously diabetic NOD females appears to model intrauterine growth restriction and preeclampsia in human diabetic pregnancy. Links between NK cells and autoimmunity are beginning to be understood. Their relationships during physiological stress such as pregnancy require further study.

ACKNOWLEDGMENTS

This work was supported by the Canadian Institutes for Health Research. B.A.C. is a Tier 1 Canada Research Chair.

We thank Drs. E. Leiter (The Jackson Laboratory, Bar Harbor, ME), M. van den Heuvel (University of Western Ontario, London, Ontario, Canada), C. McKerlie and Mr. C. Fleming (Mount Sinai Hospital, Toronto, Ontario, Canada) for invaluable advice, and M. Bilinski and R. Watering for technical support.

REFERENCES

1. Leiter EH: The NOD mouse: a model for insulin-dependent diabetes mellitus. *Curr Protocols Immunol* 24 (Suppl.):15.9.1–15.9.23, 1997
2. Wicker LS, Clark J, Fraser HI, Garner VE, Gonzalez-Munoz A, Healy B, Howlett S, Hunter K, Rainbow D, Rosa RL, Smink LJ, Todd JA, Peterson LB: Type 1 diabetes genes and pathways shared by humans and NOD mice. *J Autoimmun* 25 (Suppl.):29–33, 2005
3. Wicker LS, Todd JA, Peterson LB: Genetic control of autoimmune diabetes in the NOD mouse. *Annu Rev Immunol* 13:179–200, 1995
4. Hanninen A, Taylor C, Streeter PR, Stark LS, Sarte JM, Shizuru JA, Simell O, Michie SA: Vascular addressins are induced on islet vessels during insulitis in nonobese diabetic mice and are involved in lymphoid cell binding to islet endothelium. *J Clin Invest* 92:2509–2515, 1993
5. Serreze DV, Leiter EH: Defective activation of T suppressor cell function in nonobese diabetic mice: potential relation to cytokine deficiencies. *J Immunol* 140:3801–3807, 1988
6. Alard P, Manirarora JN, Parnell SA, Hudkins JL, Clark SL, Kosiewicz MM: Deficiency in NOD antigen-presenting cell function may be responsible for suboptimal CD4+CD25+ T-cell-mediated regulation and type 1 diabetes development in NOD mice. *Diabetes* 55:2098–2105, 2006
7. Wu AJ, Hua H, Munson SH, McDevitt HO: Tumor necrosis factor-alpha regulation of CD4+CD25+ T cell levels in NOD mice. *Proc Natl Acad Sci U S A* 99:12287–12292, 2002
8. Hammond KJ, Pellicci DG, Poulton LD, Naidenko OV, Scalzo AA, Baxter AG, Godfrey DI: CD1d-restricted NKT cells: an interstrain comparison. *J Immunol* 167:1164–1173, 2001
9. Poulton LD, Smyth MJ, Hawke CG, Silveira P, Shepherd D, Naidenko OV, Godfrey DI, Baxter AG: Cytometric and functional analyses of NK and NKT cell deficiencies in NOD mice. *Int Immunol* 13:887–896, 2001
10. Morishima M, Yasui H, Ando M, Nakazawa M, Takao A: Influence of genetic and maternal diabetes in the pathogenesis of visceroatrial heterotaxy in mice. *Teratology* 54:183–190, 1996
11. Morishima M, Ando M, Takao A: Visceroatrial heterotaxy syndrome in the NOD mouse with special reference to atrial situs. *Teratology* 44:91–100, 1991
12. Otani H, Tanaka O, Tatewaki R, Naora H, Yoneyama T: Diabetic environment and genetic predisposition as causes of congenital malformations in NOD mouse embryos. *Diabetes* 40:1245–1250, 1991
13. Yang J, Cummings EA, O'Connell C, Jangaard K: Fetal and neonatal outcomes of diabetic pregnancies. *Obstet Gynecol* 108:644–650, 2006
14. Cordero L, Treuer SH, Landon MB, Gabbe SG: Management of infants of diabetic mothers. *Arch Pediatr Adolesc Med* 152:249–254, 1998
15. Evers IM, Nikkels PG, Sikkema JM, Visser GH: Placental pathology in women with type 1 diabetes and in a control group with normal and large-for-gestational-age infants. *Placenta* 24:819–825, 2003
16. Mayhew TM: Enhanced fetoplacental angiogenesis in pre-gestational diabetes mellitus: the extra growth is exclusively longitudinal and not accompanied by microvascular remodelling. *Diabetologia* 45:1434–1439, 2002
17. Jauniaux E, Burton GJ: Villous histomorphometry and placental bed biopsy investigation in type I diabetic pregnancies. *Placenta* 27:468–474, 2006
18. Evers IM, de Valk HW, Visser GH: Risk of complications of pregnancy in women with type 1 diabetes: nationwide prospective study in the Netherlands. *BMJ* 328:915, 2004
19. Vinatier D, Monnier JC: Pre-eclampsia: physiology and immunological aspects. *Eur J Obstet Gynecol Reprod Biol* 61:85–97, 1995
20. Anne Croy B, van den Heuvel MJ, Borzychowski AM, Tayade C: Uterine natural killer cells: a specialized differentiation regulated by ovarian hormones. *Immunol Rev* 214:161–185, 2006
21. Li XF, Charnock-Jones DS, Zhang E, Hiby S, Malik S, Day K, Licence D, Bowen JM, Gardner L, King A, Loke YW, Smith SK: Angiogenic growth factor messenger ribonucleic acids in uterine natural killer cells. *J Clin Endocrinol Metab* 86:1823–1834, 2001
22. Hanna J, Goldman-Wohl D, Hamani Y, Avraham I, Greenfield C, Natanson-Yaron S, Prus D, Cohen-Daniel L, Arnon TI, Manaster I, Gazit R, Yutkin V, Benharroch D, Porgador A, Keshet E, Yagel S, Mandelboim O: Decidual NK cells regulate key developmental processes at the human fetal-maternal interface. *Nat Med* 12:1065–1074, 2006
23. Greenwood JD, Minhas K, di Santo JP, Makita M, Kiso Y, Croy BA: Ultrastructural studies of implantation sites from mice deficient in uterine natural killer cells. *Placenta* 21:693–702, 2000
24. Chantakru S, Miller C, Roach LE, Kuziel WA, Maeda N, Wang WC, Evans SS, Croy BA: Contributions from self-renewal and trafficking to the uterine NK cell population of early pregnancy. *J Immunol* 168:22–28, 2002
25. Lynch L, Golden-Mason L, Eogan M, O'Herlihy C, O'Farrelly C: Cells with haematopoietic stem cell phenotype in adult human endometrium: relevance to infertility? *Hum Reprod* 22:919–926, 2007
26. van den Heuvel MJ, Horrocks J, Bashar S, Hatta K, Burke S, Evans SS, Croy BA, Tekpetey FR: Periovulatory increases in tissue homing potential of circulating CD56 (bright) cells are associated with fertile menstrual cycles. *J Clin Endocrinol Metab* 90:3606–3613, 2005
27. King A, Burrows T, Verma S, Hiby S, Loke YW: Human uterine lymphocytes. *Hum Reprod Update* 4:480–485, 1998
28. Prophet EB, Mills B, Arrington JB, Sobin LH: *Armed Forces Institute of Pathology Laboratory Methods in Histotechnology*. Washington, DC, American Registry of Pathology, 1992
29. Wang WC, Goldman LM, Schleider DM, Appenheimer MM, Subjeck JR, Repasky EA, Evans SS: Fever-range hyperthermia enhances L-selectin-dependent adhesion of lymphocytes to vascular endothelium. *J Immunol* 160:961–969, 1998
30. Xie X, He H, Colonna M, Seya T, Takai T, Croy BA: Pathways participating

in activation of mouse uterine natural killer cells during pregnancy. *Biol Reprod* 73:510–518, 2005
31. Ashkar AA, Croy BA: Interferon-gamma contributes to the normalcy of murine pregnancy. *Biol Reprod* 61:493–502, 1999
32. Loeken MR: Advances in understanding the molecular causes of diabetes-induced birth defects. *J Soc Gynecol Investig* 13:2–10, 2006
33. Esadeg S, He H, Pijnenborg R, Van Leuven F, Croy BA: Alpha-2 macroglobulin controls trophoblast positioning in mouse implantation sites. *Placenta* 24:912–921, 2003
34. Ashkar AA, Black GP, Wei Q, He H, Liang L, Head JR, Croy BA: Assessment of requirements for IL-15 and IFN regulatory factors in uterine NK cell differentiation and function during pregnancy. *J Immunol* 171:2937–2944, 2003
35. van den Heuvel MJ, Horrocks J, Bashar S, Taylor S, Burke S, Hatta K, Lewis JE, Croy BA: Menstrual cycle hormones induce changes in functional interactions between lymphocytes and decidual vascular endothelial cells. *J Clin Endocrinol Metab* 90:2835–2842, 2005
36. Guimond MJ, Wang B, Croy BA: Engraftment of bone marrow from severe combined immunodeficient (SCID) mice reverses the reproductive deficits in natural killer cell-deficient tg epsilon 26 mice. *J Exp Med* 187:217–223, 1998
37. Rivard A, Silver M, Chen D, Kearney M, Magner M, Annex B, Peters K, Isner JM: Rescue of diabetes-related impairment of angiogenesis by intramuscular gene therapy with adeno-VEGF. *Am J Pathol* 154:355–363, 1999
38. Wang C, Umesaki N, Nakamura H, Tanaka T, Nakatani K, Sakaguchi I, Ogita S, Kaneda K: Expression of vascular endothelial growth factor by granulated metrial gland cells in pregnant murine uteri. *Cell Tissue Res* 300:285–293, 2000
39. Tayade C, Hilchie D, He H, Fang Y, Moons L, Carmeliet P, Foster RA, Croy BA: Genetic deletion of placenta growth factor in mice alters uterine NK cells. *J Immunol* 178:4267–4275, 2007
40. Grunewald M, Avraham I, Dor Y, Bachar-Lustig E, Itin A, Yung S, Chimenti S, Landsman L, Abramovitch R, Keshet E: VEGF-induced adult neovascularization: recruitment, retention, and role of accessory cells. *Cell* 124:175–189, 2006
41. Shultz LD, Schweitzer PA, Christianson SW, Gott B, Schweitzer IB, Tennent B, McKenna S, Mobraaten L, Rajan TV, Greiner DL: Multiple defects in innate and adaptive immunologic function in NOD/LtSz-scid mice. *J Immunol* 154:180–191, 1995
42. Ancelin M, Buteau-Lozano H, Meduri G, Osborne-Pellegrin M, Sordello S, Plouet J, Perrot-Applanat M: A dynamic shift of VEGF isoforms with a transient and selective progesterone-induced expression of VEGF189 regulates angiogenesis and vascular permeability in human uterus. *Proc Natl Acad Sci U S A* 99:6023–6028, 2002
43. Boehm U, Klamp T, Groot M, Howard JC: Cellular responses to interferon-gamma. *Annu Rev Immunol* 15:749–795, 1997
44. Ashkar AA, di Santo JP, Croy BA: Interferon gamma contributes to initiation of uterine vascular modification, decidual integrity, and uterine natural killer cell maturation during normal murine pregnancy. *J Exp Med* 192:259–270, 2000
45. Rodacki M, Svoren B, Butty V, Besse W, Laffel L, Benoist C, Mathis D: Altered natural killer cells in type 1 diabetic patients. *Diabetes* 56:177–185, 2007
46. Ogasawara K, Hamerman JA, Hsin H, Chikuma S, Bour-Jordan H, Chen T, Pertel T, Carnaud C, Bluestone JA, Lanier LL: Impairment of NK cell function by NKG2D modulation in NOD mice. *Immunity* 18:41–51, 2003
47. Yang X, Karin N, Tisch R, Steinman L, McDevitt HO: Inhibition of insulitis and prevention of diabetes in nonobese diabetic mice by blocking L-selectin and very late antigen 4 adhesion receptors. *Proc Natl Acad Sci U S A* 90:10494–10498, 1993
48. Kruse A, Merchant MJ, Hallmann R, Butcher EC: Evidence of specialized leukocyte-vascular homing interactions at the maternal/fetal interface. *Eur J Immunol* 29:1116–1126, 1999
49. Denis MC, Mahmood U, Benoist C, Mathis D, Weissleder R: Imaging inflammation of the pancreatic islets in type 1 diabetes. *Proc Natl Acad Sci U S A* 101:12634–12639, 2004